IEEE Access
Multidisciplinary ⋮ Rapid Review ⋮ Open Access Journal

Received July 28, 2019, accepted August 7, 2019, date of publication August 19, 2019, date of current version September 9, 2019.

Digital Object Identifier 10.1109/ACCESS.2019.2936100

Adaptive Minimum-Entropy Hybrid Compensation for Compound Faults of Non-Gaussian Stochastic Systems

KAIYU HU[1], FUYANG CHEN[1], ZIAN CHENG[1], AND CHANGYUN WEN[2], (Fellow, IEEE)
[1]College of Automation Engineering, Nanjing University of Aeronautics and Astronautics, Nanjing 211106, China
[2]School of Electrical and Electronic Engineering, Nanyang Technological University, Singapore 639798

Corresponding author: Kaiyu Hu (hukaiyuluran@126.com)

This work was supported in part by the National Natural Science Foundation of China under Grant 61533009.

ABSTRACT This study investigated minimum-entropy hybrid fault-tolerant control (FTC) theory for non-Gaussian stochastic systems with compound faults. After fuzzy linearization for the singular systems, the output probability density function (PDF) is generated by rational square root B-splines. To deal with the compound faults consisting of single sensor fault and intermittent multiple actuator faults, an active-passive hybrid adaptive FTC scheme is proposed: A passive compensation function can directly reconstruct the algorithm to mask the sensor fault; then, actuator fault estimation accurately tracks the multiple actuator faults. Hence, the hybrid FTC combines estimated information and passive compensation simultaneously implements active actuator fault repair and passive sensor fault shielding. A novel variable parameter algorithm that mimics animal predation behavior is designed and incorporated into learning rates, making the controller more sensitive to the incipient deviations in actuator faults. Finally, with the optimal indicators containing entropy and mean of non-Gaussian PDF, the minimum-entropy FTC is achieved. Lyapunov and indicator functions prove the stability, simulation verifies the effectiveness of the methods.

INDEX TERMS Control theory, fault-tolerant control, compound faults, entropy, stochastic systems.

I. INTRODUCTION

Non-Gaussian stochastic distribution control (SDC) has a wide range of application scenarios; it can describe industrial processes such as parallel vibration tables, aerospace engine tail flames, and pulper fiber distribution control [1]–[4]. Studying such systems' fault diagnosis (FD) and fault-tolerant control (FTC) can compensate for the faults that cannot be displayed by traditional system outputs, provide new ideas for anti-laser hypersonic vehicles and industrial process safety design. There are some under consequential issues in this research area, including FTC of compound faults, estimation of incipient or intermittent faults, and optimal control when the expected output is unknown.

Multiple or compound faults are different types of faults occurring simultaneo4usly, or the same fault occurring simultaneously at different internal locations [5], [6]. It is difficult for a single FTC algorithm to compensate for compound faults. Therefore, special FTC schemes are needed to deal with such faults. In [7], the problem of diagnosing compound faults over time was solved using a framework based on a coupled-factorial hidden Markov model. In [8], a frequency-blind deconvolution algorithm based on an adaptive generalized morphological filter was proposed for extracting useful signals from signals contaminated by compound faults. In [9], a nonlinear FTC and multiple-sensor FD approach for longitudinal dynamics of hypersonic vehicles was designed. In [10], a composite loop for FTC under compound faults was subsequently developed, where a newly developed multivariable integral sliding-mode control was integrated. In [11], an improved fast-spectrum kurtosis method combined with variational mode decomposition was proposed to improve the tracking accuracy for compound faults. In [12], an exponentially weighted moving average control chart was constructed to diagnose compound faults at an early stage. In [13], a low-complexity state feedback FTC scheme that guarantees prescribed performance was designed for actuator

The associate editor coordinating the review of this article and approving it for publication was Feiqi Deng.

and component faults. In [14], an FTC scheme with higher order sliding-mode-based observers was proposed to provide continuous drive operation regardless of any sensor faults. In [15], a robust adaptive FTC was designed to address the tracking control problem with prescribed performance guarantees for a system subject to unknown inertia properties, actuator faults, and saturation nonlinearities. In [16]–[18], the actuator and sensor compound faults were considered simultaneously when designing controllers, and a similar approach was also applied to systems with multiple complex conditions. Based on the previous research, part of this study was conducted to solve the problem of FTC for actuator-sensor compound faults.

A background of incipient and intermittent faults represents the early signs before large permanent faults occur. In [19], under the principal component analysis framework, a new data-driven FD method was proposed to extract the incipient faults. In [20], an interval sliding mode observer and an incipient sensor fault detection method were proposed for a class of nonlinear control systems with observer unmatched uncertainties. In [21], a new method for FD of transformers with dissolved gas analysis was used to detect incipient faults in oil-cooled transformers. In [22], the realization form of multiplicative faults was first studied with the aid of coprime factorization techniques. Then, a fault-tolerant margin was designed in the closed-loop setup, aiming at characterizing fault induced performance degradation. In [23], non-fragile FTC was addressed for a class of nonlinear jump systems with intermittent multiple actuator faults. In [24], a method based on chaotic spread-spectrum sequence was proposed for synchronous online diagnosis of intermittent faults for complex networks, such as aircraft power systems. In [25], event-triggered filtering and intermittent fault detection problems were investigated for a class of time-varying systems with stochastic parameter uncertainty and sensor saturation. In [26], output feedback controller and linear matrix inequality (LMI) were designed for the Takagi-Sugeno (T-S) fuzzy systems with input parameter uncertainties, exogenous disturbances, measurement noise, and multiple intermittent faults. These research results motivated part of the present study to solve the problem of FTC of intermittent time-varying step faults involving incipient faults.

Some research results have been obtained in FD and FTC of non-Gaussian stochastic systems. In [27], a generalized correntropy filter-based diagnosis and repair strategy were proposed for stochastic systems with heavy-tailed distributed non-Gaussian noise. In [28], T-S fuzzy theory was used for non-Gaussian stochastic systems; a sliding-mode algorithm compensated for the fault impacts. In [29], algorithms were proposed for singular time-delay systems with non-Gaussian stochastic output and probability density function (PDF) approximation error. In [30], an adaptive observer and novel fault-tolerant proportional-integral controller were designed because of the singular and delay of non-Gaussian stochastic systems. In [31], using the rational square-root B-spline model for the shape control of the system output PDF, a nonlinear adaptive observer-based FD algorithm was proposed to diagnose the fault.

The motivation of minimum-entropy SDC is that the expected output PDF is unknown [31]. We design a novel hybrid FTC scheme, where non-Gaussian stochastic systems can achieve the optimal FTC of entropy index under the compound faults and unknown expected PDF conditions. The main contributions of this study include:

1) Construction of fuzzy singular non-Gaussian systems and a performance index with mean and entropy, designing fusion adaptive control combining fuzzy premise variables and fault information to achieve the minimum-entropy optimal control.

2) Design of an active-passive hybrid FTC scheme. When sensor faults occur, passive minimum-entropy FTC without detection is achieved; when sensor-actuator compound faults occur, the scheme estimates and actively compensates actuator faults while shielding sensor faults.

3) Design of a novel variable parameter algorithm imitating animal predation behavior, making the systems more sensitive to time-varying step faults with incipient deviation, improving the estimation and FTC performance.

This paper is organized as follows. Section II establishes the general non-Gaussian stochastic systems with compo-und faults and provides the fault expressions. Section III. A discusses the design of an adaptive observer for actuator time-varying step faults, Section III. B discusses the design of a hybrid minimum-entropy FTC scheme, and Section III. C covers the design of a variable-parameter prey algorithm. Section IV describes the simulation conducted to verify the effectiveness of all methods.

II. MODEL SYSTEMS AND FAULTS

We take $\gamma(y, u(t))$ as the output PDF of a non-Gaussian stochastic system, where y is a stochastic variable defined in the real interval $[a, b]$. Then, a class of compound faults with actuator and sensor faults is introduced, so the system expression under one of the T-S fuzzy rules is as follows:

The ith rule: *IF* $\varpi_1(t)$ *is* β_{i1}, *and* ..., *and* $\varpi_\iota(t)$ *is* $\beta_{i\iota}$, *THEN*:

$$\begin{cases} E\dot{x}(t) = A_i x(t) + B_i u(t) + N_i F_{tvs}(t) \\ V(t) = D_i x(t) \end{cases} \tag{1}$$

$$\sqrt{\gamma(y+c, u(t))} = \frac{C(y+c)V(t)}{\sqrt{V^T(t)\Sigma_i V(t)}} \tag{2}$$

where $\varpi_\eta(\eta = 1, \ldots, \iota)$ are the premise variables, ι is the number of premise variables, and $\beta_{i\eta}(i = 1, \ldots, \bar{n})$ are the fuzzy sets.

The membership function for each linear modal is as follows:

$$\begin{cases} h_i(\varpi(t)) = \prod_{\eta=1}^{\iota} \beta_{i\eta}(\varpi(t)) / \sum_{i=1}^{\bar{n}} \prod_{\eta=1}^{\iota} \beta_{i\eta}(\varpi(t)) \geq 0 \\ \sum_{i=1}^{\bar{n}} h_i(\varpi(t)) = 1 \end{cases} \tag{3}$$

Therefore the non-Gaussian nonlinear stochastic systems after fuzzy approximation is expressed as follows:

$$\begin{cases} E\dot{x}(t) = \sum_{i=1}^{\bar{n}} h_i(\varpi(t))(A_i x(t) + B_i u(t) + N_i F_{tvs}(t)) \\ V(t) = \sum_{i=1}^{\bar{n}} h_i(\varpi(t)) D_i x(t) \end{cases} \tag{4}$$

$$\sqrt{\gamma(y+c, u(t))} = \sum_{i=1}^{\bar{n}} h_i(\varpi(t))\Lambda_i C(y+c)V(t) \tag{5}$$

In (4) and (5), $x(t) \in R^{n\times 1}$ is the state vector, $V(t) \in R^{(n-1)\times 1}$ is the system output weight vector, $u(t) \in R^{m\times 1}$ is the control input vector, $c \in R$ is the single sensor initial fault, and $F_{tvs}(t) \in R^{m\times 1}$ is the vector with multiple actuator faults. Actuator faults are a class of intermittent time-varying step faults with the incipient fault interval defined by literature [19], and satisfy:

$$F_{tvs}(t) = \begin{cases} F_\sigma(t), & t \in (t_{\sigma 1}, t_{\sigma 2}] \\ 0, & otherwise \end{cases} \tag{6}$$

$$F_\sigma(t) = \begin{cases} F_{\sigma,inc}(t), & t \in (t_{\sigma 1}, t_{\sigma 3}] \\ F_{\sigma,non-inc}(t), & t \in (t_{\sigma 3}, t_{\sigma 2}] \end{cases} \tag{7}$$

$$\begin{cases} \left\| F_{\sigma,inc}(t)/(B_i u^*(t)) \right\| \le 10\% \\ \left\| F_{\sigma,non-inc}(t)/(B_i u^*(t)) \right\| > 10\% \end{cases} \tag{8}$$

where $F_{tvs}(t)$ are the intermittent faults with step-varying characteristics; $F_\sigma(t)$ are the values in the fault time interval; $F_{\sigma,inc}(t)$ are the values in the incipient amplitude interval; $F_{\sigma,non\text{-}inc}(t)$ are the values in the residual amplitude interval; $\sigma = 1, \ldots, \sigma_0$ is the number of fault windows; and $\|B_i u^*(t)\|$ is the minimum norm when no compound faults occur. The judgment method is in Remark 2.

The system parameter matrices and their dimensions satisfy: $A_i \in R^{n\times n}$, $B_i \in R^{n\times m}$, $D_i \in R^{(n-1)\times n}$, $E \in R^{n\times n}$, and $N_i \in R^{n\times n}$. rank$(E) = q < n$, where E is the singular matrix. Equation (5) is a PDF static model fitted by the rational square root B-spline functions, where:

$$\Lambda_i = 1/\sqrt{V^T(t)(\Sigma_i + \Delta\Sigma_i)V(t)} \tag{9}$$

$$\begin{aligned} \Sigma_i + \Delta\Sigma_i &= \int_a^b C^T(y+c)U_i C(y+c)dy \\ &= \int_a^b (C^T(y) + \Delta C^T)U_i(C(y) + \Delta C)dy \\ &= \int_a^b (C^T(y)U_i C(y) + C^T(y)U_i\Delta C \\ &\quad + \Delta C^T U_i C(y) + \Delta C^T U_i \Delta C)dy \end{aligned} \tag{10}$$

$$\begin{aligned} C(y+c) &= [B_1(y+c)\ B_2(y+c)\ \ldots\ B_n(y+c)] \\ &= [B_1(y) + \Delta B_1\ B_2(y) + \Delta B_2\ \ldots\ B_n(y) + \Delta B_n] \\ &= [B_1(y)\ \ B_2(y) \ldots B_n(y)] + [\Delta B_1\ \Delta B_2\ \ldots\ \Delta B_n] \\ &= C(y) + \Delta C \end{aligned} \tag{11}$$

$$V(t) = [v_1(t)\ v_2(t)\ \ldots\ v_n(t)]^T \tag{12}$$

$$\Sigma_i = \int_a^b C^T(y)U_i C(y)dy \tag{13}$$

$$\begin{aligned} \Delta\Sigma_i = \int_a^b &(C^T(y)U_i\Delta C + \Delta C^T U_i C(y) \\ &+ \Delta C^T U_i \Delta C)dy \end{aligned} \tag{14}$$

$v_j(u(t))(j= 1, 2, \ldots, n)$ are the weights associated with input $u(t)$, $B_j(y+c)(j = 1, 2, \ldots, n)$ are the predetermined basis functions, and n is the number of basis functions. U_i is an independently set parameter matrix that compensates for interpolation errors with the changes of premise variables. $C(y) = [B_1(y), B_2(y), \ldots, B_n(y)]$ is the basis function vector for sensorless faults, and ΔC and $\Delta \Sigma_i$ are the effect of sensor initial fault on the basis function vector.

Remark 1: There are multiple actuator faults and a single sensor fault in the system, so in this paper, the description is: "actuator faults" and "sensor fault."

Assumption 1: System (4) is pulseless and regular, i.e. rank$E$= deg($| sE - Ai |$) and $| sE - Ai | \neq 0$.

According to Assumption 1, two non-singular matrices Q_i and P_i can be found and satisfy

$$\sum_{i=1}^{\bar{n}} h_i(\varpi(t))Q_i E P_i = \begin{bmatrix} I_q & 0 \\ 0 & 0 \end{bmatrix} \tag{15}$$

$$\sum_{i=1}^{\bar{n}} h_i(\varpi(t))Q_i A_i P_i = \sum_{i=1}^{\bar{n}} h_i(\varpi(t)) \begin{bmatrix} A_{i1} & 0 \\ 0 & I_{n-q} \end{bmatrix} \tag{16}$$

where $Q_i, P_i \in R^{n\times n}$, $A_{i1} \in R^{q\times q}$, and I_q is a q-order unit matrix.

Set the following state transformation

$$x(t) = \sum_{i=1}^{\bar{n}} h_i(\varpi(t))P_i \begin{bmatrix} x_1(t) \\ x_2(t) \end{bmatrix} \tag{17}$$

where $x_1(t) \in R^{q\times 1}$, $x_2(t) \in R^{(n-q)\times 1}$; hence, systems (4) and (5) can be transformed into

$$\begin{cases} \dot{x}_1(t) = \sum_{i=1}^{\bar{n}} h_i(\varpi(t))(A_{i1}x_1(t) + B_{i1}u(t) + N_{i1}F_{tvs}(t)) \\ x_2(t) = \sum_{i=1}^{\bar{n}} h_i(\varpi(t))(-B_{i2}u(t) - N_{i2}F_{tvs}(t)) \\ V(t) = \sum_{i=1}^{\bar{n}} h_i(\varpi(t))(D_{i1}x_1(t) + D_{i2}x_2(t)) \\ \sqrt{\gamma(y+c, u(t))} = \sum_{i=1}^{\bar{n}} h_i(\varpi(t))\Lambda_i(C(y) + \Delta C)V(t) \end{cases} \tag{18}$$

where $B_{i1}, N_{i1} \in R^{q\times m}$, $B_{i2}, N_{i2} \in R^{(n-q)\times m}$, $D_{i1} \in R^{(n-1)\times q}$, and $D_{i2} \in R^{(n-1)\times(n-q)}$, and satisfy $Q_i B_i = [\,B_{i1}^T\ B_{i2}^T\,]^T$, $Q_i N_i = [\,N_{i1}^T\ N_{i2}^T\,]^T$, $D_i P_i = [\,D_{i1}\ D_{i2}\,]$.

The model does not change after the state transition, so the systems (4) to (5) and (18) are equivalent.

III. FTC SCHEME DESIGN

This section designs an active-passive hybrid FTC scheme for compound faults. In an actuator fault observer, the compensation learning rates shield sensor initial fault; hence, the fusion adaptive observer tracks the actuator faults. Then, the fault-tolerant controller uses a compensation function to passively repair the sensor fault, simultaneously using the prey algorithm and estimation results to actively repair the actuator faults.

Remark 2: The sensor initial fault c is the fault being born with sensor, it is simple and does not need to design an independent observer. Engineers can determine the indirect effects of such faults based on measurable functions containing c-information such as feedback errors. Because of the complex errors produced by the environment, fault c is difficult to separate from the output measured value y. We use the observer residual with c-information design algorithms to indirectly shield c on actuator fault estimation and active FTC. In short, hybrid FTC has automatic shielding function for partial faults compared with prior art.

A. FAULT ESTIMATION

This section describes the design of an adaptive observer to estimate the actuator faults in non-Gaussian stochastic systems in order to subsequently implement the actuator faults and active FTC in the hybrid FTC. The observer is as follows:

$$\begin{cases} \dot{x}_{1m}(t) = \sum_{i=1}^{\bar{n}} h_i(\varpi(t))(A_{i1}x_{1m}(t) + B_{i1}u(t) \\ \qquad + N_{i1}\hat{F}_{tvs}(t) + K_i\varepsilon_m(t)) \\ x_{2m}(t) = \sum_{i=1}^{\bar{n}} h_i(\varpi(t))(-B_{i1}u(t) - N_{i2}\hat{F}_{tvs}(t)) \\ V_m(t) = \sum_{i=1}^{\bar{n}} h_i(\varpi(t))(D_{i1m}x_{1m}(t) + D_{i2m}x_{2m}(t)) \\ \sqrt{\gamma_m(y+c, u(t))} = \sum_{i=1}^{\bar{n}} h_i(\varpi(t))\Lambda_{im}(C(y) + \Delta C)V_m(t) \\ \varepsilon_m(t) = \int_a^b \sigma(y+c)[\sqrt{\gamma(y+c, u(t))} - \sqrt{\gamma_m(y+c, u(t))}]dy \end{cases} \tag{19}$$

$$\dot{\hat{F}}_{tvs}(t) = \sum_{i=1}^{\bar{n}} h_i(\varpi(t))(-prey(R_i)\hat{F}_{tvs}(t) + r_{i,c}\varepsilon_m(t)) \tag{20}$$

where $x_{jm}(t)(j = 1, 2)$ are the state estimation values, $\varepsilon_m(t)$ is the residual signal, K_i is an observer gain, and $prey(R_i)$, $r_{i,c}$ are the fusion adaptive learning matrices with a certain dimension. $prey(R_i)$ contains information about actuator fault estimation and fuzzy premise variables; $r_{i,c}$ contains information about fuzzy premise variables and residual. $\hat{F}_{tvs}(t)$ is the estimation of $F_{tvs}(t)$.

$$\Lambda_{im} = 1/\sqrt{V_m^T(t)(\Sigma_i + \Delta\Sigma_i)V_m(t)} \tag{21}$$

Remark 3: $prey(\cdot)$ is the prey algorithm that increases an independent switching dimension of the learning rates and does not affect the stability proof. Compared with the state-of-art in [31], prey algorithm increases the adjustment freedom of learning rates and makes the systems adapt to more environmental factors. This algorithm's characteristics are described in Section III.C.

According to (19), (20) and (21), the observation error and fault estimation error are

$$e_{1m}(t) = x_1(t) - x_{1m}(t) \tag{22}$$

$$\tilde{F}_{tvs}(t) = F_{tvs}(t) - \hat{F}_{tvs}(t) \tag{23}$$

The residual signal can be expressed as

$$\begin{aligned} \varepsilon_m(t) &= \int_a^b \sigma(y+c)[\sqrt{\gamma(y+c, u(t))} - \sqrt{\gamma_m(y+c, u(t))}]dy \\ &= \sum_{i=1}^{\bar{n}} h_i(\varpi(t))(\Lambda_i(\Gamma + \Delta\Gamma)V(t) \\ &\quad + \Lambda_{im}(\Gamma + \Delta\Gamma)D_{i1}e_{1m}(t) - \Lambda_{im}(\Gamma \\ &\quad + \Delta\Gamma)D_{i2}N_{i2}\tilde{F}(t) - \Lambda_{im}(\Gamma + \Delta\Gamma)V(t)) \end{aligned} \tag{24}$$

where

$$\begin{aligned} \Gamma + \Delta\Gamma &= \int_a^b \sigma(y+c)(C(y) + \Delta C)dy \\ &= \int_a^b \sigma(y+c)C(y)dy + \int_a^b \sigma(y+c)\Delta C dy \end{aligned} \tag{25}$$

$$\begin{cases} \Gamma = \int_a^b \sigma(y+c)C(y)dy \\ \Delta\Gamma = \int_a^b \sigma(y+c)\Delta C dy \end{cases} \tag{26}$$

The first derivative of fault estimation error is

$$\begin{aligned} \dot{\tilde{F}}_{tvs}(t) &= -\dot{\hat{F}}_{tvs}(t) \\ &= \sum_{i=1}^{\bar{n}} h_i(\varpi(t))(prey(R_i)\hat{F}_{tvs}(t) - r_{i,c}\varepsilon_m(t)) \\ &= \sum_{i=1}^{\bar{n}} h_i(\varpi(t))\{prey(R_i)F_{tvs}(t) - prey(R_i)\tilde{F}_{tvs}(t) \\ &\quad - r_{i,c}[\Lambda_{im}(\Gamma + \Delta\Gamma)D_{i1}e_{1m}(t) \\ &\quad - \Lambda_{im}(\Gamma + \Delta\Gamma)D_{i2}N_{i2}\tilde{F}_{tvs}(t)] \\ &\quad - r_{i,c}[\Lambda_i(\Gamma + \Delta\Gamma)V(t) - \Lambda_{im}(\Gamma + \Delta\Gamma)V(t)]\} \end{aligned} \tag{27}$$

According to (27), the first derivative of error $e_{1m}(t)$ is further obtained:

$$\begin{aligned} \dot{e}_{1m}(t) &= \dot{x}_1(t) - \dot{x}_{1m}(t) \\ &= \sum_{i=1}^{\bar{n}} h_i(\varpi(t))\{[A_{i1} - L_{i1}(\Gamma + \Delta\Gamma)D_{i1}]e_{1m}(t) \\ &\quad + [N_{i1} + L_{i1}(\Gamma + \Delta\Gamma)D_{i2}N_{i2}]\tilde{F}_{tvs}(t) + L_{i1}(\Gamma \\ &\quad + \Delta\Gamma)V(t)\Lambda_i\lambda_1(\|V(t)\| - \|\hat{V}_m(t)\|)\} \end{aligned}$$

$$= \sum_{i=1}^{\bar{n}} h_i(\varpi(t))\{[A_{i1} - L_{i1}(\Gamma + \Delta\Gamma)D_{i1}]e_{1m}(t) + [N_{i1} + L_{i1}(\Gamma + \Delta\Gamma)D_{i2}N_{i2}]\tilde{F}_{tvs}(t) + L_{i1}(\Gamma + \Delta\Gamma)h_1(t)\} \tag{28}$$

where

$$K_{i1} = L_{i1}/\Lambda_{im} \tag{29}$$

$$h_1(t) = V(t)\Lambda_i\lambda_1(\|V(t)\| - \|V_m(t)\|) \tag{30}$$

According to the literature [32], inequality (31) can be obtained as

$$\begin{aligned} h_1^T(t)h_1(t) &\leq \sum_{i=1}^{\bar{n}} h_i(\varpi(t))(T_2\|D_{i0}\|/\sqrt{\|\Sigma_i + \Delta\Sigma_i\|})^2 \\ &\quad \times [e_{1m}^T(t)e_{1m}(t) + \tilde{F}_{tvs}^T(t)N_{i2}^T N_{i2}\tilde{F}_{tvs}(t)] \\ &= \sum_{i=1}^{\bar{n}} h_i(\varpi(t))[\alpha_1 e_{1m}^T(t)e_{1m}(t) \\ &\quad + \alpha_1\tilde{F}_{tvs}^T(t)N_{i2}^T N_{i2}\tilde{F}_{tvs}(t)] \end{aligned} \tag{31}$$

where

$$D_{i0} = D_iP_i = [D_{i1}D_{i2}] \tag{32}$$

$$\alpha_1 = (T_2\|D_{i0}\|)^2/\|\Sigma_i + \Delta\Sigma_i\| \tag{33}$$

Remark 4: A positive threshold τ_1 of approximately zero can describe the effect of the sensor initial fault c on the residual ε_m. The absolute value of the residual exceeds τ_1 to indicate the influence of c in the systems. If not exceeds, it indicates that there is no impact of c in the systems. A positive threshold τ_2 is the actuator faults judgment threshold. If the norm of multiple actuator fault vector exceeds τ_2, the systems determine that actuator faults have occurred.

Assumption 2: $\forall t \geq 0$, actuator faults and sensor fault satisfy

$$\begin{cases} \left\|\tilde{F}_{tvs}(t)\right\| \leq M \\ \|F_{tvs}(t)\| \leq 0.5M \\ c \leq M_c \end{cases} \tag{34}$$

where M and Mc are the positive constants. The integral interval $[a, b]$ satisfies

$$\begin{cases} a \leq \min\{y + c\} \\ b \geq \max\{y + c\} \end{cases} \tag{35}$$

Theorem 1: For the suitable parameters $\kappa > 0$, $\mu > 0$, $\alpha_1 > 0$, and $L_{i2,c}$, there exists a matrix $Y_1 = Y_1^{\mathrm{T}} > 0$ that satisfies the following inequality:

$$\Xi = \begin{bmatrix} \Phi_i + \kappa I & Y_1G_i - [L_{i2,c}(\Gamma + \Delta\Gamma)D_{i1}]^T & -Y_1L_{i1}(\Gamma + \Delta\Gamma) & 0 \\ * & -2[prey(R_i) - L_{i2,c}(\Gamma + \Delta\Gamma)D_{i2}N_{i2}] & -L_{i2,c}(\Gamma + \Delta\Gamma) & \frac{\sqrt{\alpha_1}}{\mu}N_{i2}^T \\ * & * & -\frac{1}{\mu^2}I & 0 \\ * & * & * & -I \end{bmatrix} < 0 \tag{36}$$

Then, the error system (28) is stable, where

$$\Phi_i = (A_{i1} - L_{i1}(\Gamma + \Delta\Gamma)D_{i1})^T Y_1 + Y_1(A_{i1} - L_{i1}(\Gamma + \Delta\Gamma)D_{i1}) + \frac{\alpha_1}{\mu^2}I \tag{37}$$

$$G_i = N_{i1} + L_{i1}(\Gamma + \Delta\Gamma)D_{i2}N_{i2} \tag{38}$$

$$r_{i,c} = L_{i2,c}\sqrt{V_m^T(t)(\Sigma_i + \Delta\Sigma_i)V_m(t)} \tag{39}$$

$$L_{i2,c} = l_{i2} + \Gamma_1\varepsilon_n\Gamma_2 \tag{40}$$

$$\varepsilon_n = \begin{cases} 0, & \|\varepsilon_m\| \leq \tau_1 \\ \varepsilon_m, & \|\varepsilon_m\| > \tau_1 \end{cases} \tag{41}$$

$L_{i2,c}$ is a fusion passive compensation function for the sensor initial fault. Γ_1 and Γ_2 are the shielding parameters with appropriate dimensions.

Proof: Select the Lyapunov function as:

$$\begin{aligned} \Pi(t) = \sum_{i=1}^{\bar{n}} h_i(\varpi(t))\{&e_{1m}^T(t)Y_1e_{1m}(t) + \tilde{F}_{tvs}^T(t)\tilde{F}_{tvs}(t) \\ &+ \frac{1}{\mu^2}\int_0^t [\alpha_1(e_{1m}^T(\tau)e_{1m}(\tau) + \tilde{F}_{tvs}^T(\tau)N_{i2}^T N_{i2}\tilde{F}_{tvs}(\tau)) \\ &- h_1^T(\tau)h_1(\tau)]d\tau\} \end{aligned} \tag{42}$$

The first derivative of this Lyapunov function is:

$$\begin{aligned} \dot{\Pi}(t) &= \sum_{i=1}^{\bar{n}} h_i(\varpi(t))[\dot{e}_{1m}^T(t)Y_1e_{1m}(t) + e_{1m}^T(t)Y_1\dot{e}_{1m}(t) \\ &\quad + 2\tilde{F}_{tvs}(t)^T\dot{\tilde{F}}_{tvs}(t) + \frac{\alpha_1}{\mu^2}(e_{1m}^T(t)e_{1m}(t) \\ &\quad + \tilde{F}_{tvs}(t)^T N_{i2}^T N_{i2}\tilde{F}_{tvs}(t)) - \frac{1}{\mu^2}h_1^T(t)h_1(t)] \\ &= \sum_{i=1}^{\bar{n}} h_i(\varpi(t))\{e_{1m}^T(t)[(A_{i1} - L_{i1}(\Gamma + \Delta\Gamma)D_{i1})^T Y_1 \\ &\quad + Y_1(A_{i1} - L_{i1}(\Gamma + \Delta\Gamma)D_{i1})]e_{1m}(t) \\ &\quad + 2e_{1m}^T(t)Y_1G_i\tilde{F}_{tvs}(t) + 2\tilde{F}_{tvs}(t)^T L_{i2,c}(\Gamma + \Delta\Gamma)h_1 \\ &\quad + 2\tilde{F}_{tvs}(t)^T prey(R_i)F_{tvs}(t) - 2\tilde{F}_{tvs}(t)^T prey(R_i)\tilde{F}_{tvs}(t) \\ &\quad - 2\tilde{F}_{tvs}(t)^T L_{i2,c}(\Gamma + \Delta\Gamma)(D_{i1}e_{1m}(t) \\ &\quad - 2\tilde{F}_{tvs}(t)^T D_{i2}N_{i2}\tilde{F}_{tvs}(t) + \frac{\alpha_1}{\mu^2}(e_{1m}^T(t)e_{1m}(t) \\ &\quad + \tilde{F}_{tvs}(t)^T N_{i2}^T N_{i2}\tilde{F}_{tvs}(t)) - \frac{1}{\mu^2}h_1^T(t)h_1(t) \\ &\quad + 2e_{1m}^T(t)Y_1L_{i1}(\Gamma + \Delta\Gamma)h_1(t)\} \end{aligned} \tag{43}$$

By combining similar quadratic matrices, (44) is obtained:

$$\begin{aligned}\dot{\Pi}(t) = \sum_{i=1}^{\bar{n}} & h_i(\varpi(t))\{e_{1m}^T(t)[(A_{i1} - L_{i1}(\Gamma + \Delta\Gamma)D_{i1})^T Y_1 \\ & + Y_1(A_{i1} - L_{i1}(\Gamma + \Delta\Gamma)D_{i1}) + \frac{\alpha_1}{\mu^2} I]e_{1m}(t) \\ & - 2\tilde{F}_{tvs}(t)^T(prey(R_i) - L_{i2,c}(\Gamma + \Delta\Gamma)D_{i2}N_{i2} \\ & - \frac{\alpha_1}{2\mu^2} N_{i2}^T N_{i2})\tilde{F}_{tvs}(t) - \frac{1}{\mu^2} h_1^T(t)h_1(t) \\ & + 2e_{1m}^T(t)Y_1G_i\tilde{F}_{tvs}(t) - 2\tilde{F}_{tvs}(t)^T L_{i2,c}(\Gamma \\ & + \Delta\Gamma)D_{i1}e_{1m}(t) + 2e_{1m}^T(t)Y_1L_{i1}(\Gamma + \Delta\Gamma)h_1(t) \\ & + 2\tilde{F}_{tvs}(t)^T L_{i2,c}(\Gamma + \Delta\Gamma)h_1(t) \\ & + 2\tilde{F}_{tvs}(t)^T prey(R_i)F_{tvs}(t)\} \\ = \sum_{i=1}^{\bar{n}} & h_i(\varpi(t))(X^T \Xi_{i1} X + 2\tilde{F}_{tvs}(t)^T prey(R_i)F_{tvs}(t))\end{aligned} \tag{44}$$

where

$$X^T = [e_{1m}^T(t)\ \tilde{F}_{tvs}(t)^T\ h_2^T] \tag{45}$$

$$\Xi_{i1} = \begin{bmatrix} \Phi_i & Y_1G_i - (L_{i2,c}(\Gamma+\Delta\Gamma)D_{i1})^T & -Y_1L_{i1}(\Gamma+\Delta\Gamma) \\ * & \Upsilon_i & -L_{i2,c}(\Gamma+\Delta\Gamma) \\ * & * & -\frac{1}{\mu^2} I \end{bmatrix} \tag{46}$$

$$\Upsilon_i = -2[prey(R_i) - L_{i2,c}(\Gamma + \Delta\Gamma)D_{i2}N_{i2} - \frac{\alpha_1}{2\mu^2} N_{i2}^T N_{i2}] \tag{47}$$

Therefore by means of the LMI theory, (44) can satisfy the following inequality according to Assumption 2 and Theorem 1:

$$\dot{\Pi}(t) \le -\kappa \|e_{1m}(t)\|^2 + M^2 \|prey(R_i)\| \tag{48}$$

Thus, when (49) holds, we can obtain inequality (50) as follows:

$$\|e_{1m}(t)\|^2 > \frac{M^2 \|prey(R_i)\|}{\kappa} \tag{49}$$

$$\dot{\Pi}(t) \le 0 \tag{50}$$

Thence:

$$\|e_{1m}(t)\|^2 \le \min\{e_{1m}(0), \frac{M^2 \|prey(R_i)\|}{\kappa}\} = \alpha \tag{51}$$

This indicates that the estimation error (28) is stable when compound faults exist in the systems (4) and (5).□

The proof of stability in the absence of compound faults is highly similar to the preceding proof and will not be repeated. Ultimately, the observer can use LMI to accurately track actuator faults in the event of a shielding sensor fault.

B. HYBRID COMPENSATION

The FTC process should select the best compensation solution on the basis of estimation results and consider different compound fault conditions. After fault estimation, for systems (1) and (2) when the target output PDF is unknown, the FTC method of minimum Shannon entropy should be adopted, and the performance index function is constructed as follows:

$$\begin{aligned}J(V(t), u(t)) = -S_1 \int_a^b \gamma(y + c, u(t)) \ln \gamma(y + c, u(t))dy \\ + S_2[\mu - \mu_g]^2 + u^T(t)Ru(t)\end{aligned} \tag{52}$$

In (52), the first term is the output Shannon entropy; the second term is the output mean, and satisfies

$$\mu = \int_a^b (y + c)\gamma(y + c, u(t))dy \tag{53}$$

μ_g is the expected mean, the third term is the limitation on the input energy, and $R = R^T > 0$. In order to minimize the performance index, control input $u(t)$ is chosen such that J is monotonic and not increasing, i.e.: $dJ/dt < 0$.

Set J_1 and J_2 as:

$$J_1 = -S_1 \int_a^b \gamma(y + c, u(t)) \ln \gamma(y + c, u(t))dy \tag{54}$$

$$J_2 = S_2[\mu - \mu_g]^2 \tag{55}$$

By means of the performance indicator and by proving Theorem 2, it can be shown that the selection of a control algorithm ensures the stability of minimum-entropy FTC.

Theorem 2: There is a fusion adjustment parameter $\lambda_{prey,c} > 0$ and the following controller:

$$\begin{aligned}u(t)^T R\dot{u}(t) = -\lambda_{prey,c} |\mu - \mu_g| + [S_1 \int_a^b (\ln(\gamma(y \\ + c, u(t))) + 1) \sum_{i=1}^{\bar{n}} h_i(\varpi(t))W_i dy - 2S_2(\mu \\ - \mu_g) \int_a^b (y + c) \sum_{i=1}^{\bar{n}} h_i(\varpi(t))W_i dy]\dot{V}(t)\end{aligned} \tag{56}$$

where

$$\begin{aligned}W_i = 2V^T(t)(C^T(y) + \Delta C^T)(C(y) + \Delta C)\Lambda_i^2 - 2(C(y) \\ + \Delta C)V(t)V^T(t)(\Sigma_i + \Delta\Sigma_i)\Lambda_i^4\end{aligned} \tag{57}$$

Controller (56) makes mean closed-loop non-Gaussian stochastic systems achieve the stability of minimum-entropy FTC based on performance index J.

Proof: The first derivative of performance indicator J can be expressed as:

$$\frac{dJ}{dt} = \frac{dJ_1}{dt} + \frac{dJ_2}{dt} + u(t)^T R\dot{u}(t) \tag{58}$$

because

$$\begin{aligned}\gamma(y+c,u(t)) &= \sum_{i=1}^{\bar{n}} h_i(\varpi(t))\Lambda_i^2(C(y+c)V(t))^T(C(y\\&\quad+c)V(t))\\&= \sum_{i=1}^{\bar{n}} h_i(\varpi(t))\Lambda_i^2[(C(y)+\Delta C)V(t)]^T[(C(y)\\&\quad+\Delta C)V(t)]\\&= \sum_{i=1}^{\bar{n}} h_i(\varpi(t))\Lambda_i^2[V^T(t)C^T(y)C(y)V(t)\\&\quad+V^T(t)C^T(y)\Delta CV(t)\\&\quad+V^T(t)\Delta C^T C(y)V(t)\\&\quad+V^T(t)\Delta C^T\Delta CV(t)] \end{aligned}\tag{59}$$

According to Theorem 2 and (57), partial derivation (60) can be obtained:

$$\begin{aligned}W_i &= \frac{\partial\gamma(y+c,u(t))}{\partial V(t)}\\&= \frac{2V^T(t)(C^T(y)+\Delta C^T)(C(y)+\Delta C)/\Lambda_i^2}{1/\Lambda_i^4}\\&\quad-\frac{2(C(y)+\Delta C)V(t)(V^T(t)(\Sigma_i+\Delta\Sigma_i))}{1/\Lambda_i^4}\\&= 2V^T(t)(C^T(y)+\Delta C^T)(C(y)+\Delta C)\Lambda_i^2\\&\quad-2(C(y)+\Delta C)V(t)V^T(t)(\Sigma_i+\Delta\Sigma_i)\Lambda_i^4\end{aligned}\tag{60}$$

Deriving J_1 and J_2 separately, we can obtain:

$$\begin{aligned}\frac{dJ_1}{dt} &= -S_1\int_a^b\Big(\frac{\partial\gamma(y+c,u(t))}{\partial V(t)}\dot{V}(t)\ln\gamma(y+c,u(t))\\&\quad+\frac{\partial\gamma(y+c,u(t))}{\partial V(t)}\dot{V}(t)\Big)dy \qquad (61)\\&= -S_1\int_a^b(\ln\gamma(y+c,u(t))+1)\sum_{i=1}^{\bar{n}}h_i(\varpi(t))W_i dy\dot{V}(t)\end{aligned}$$

$$\frac{dJ_2}{dt} = 2S_2(\mu-\mu_g)\int_a^b(y+c)\sum_{i=1}^{\bar{n}}h_i(\varpi(t))W_i dy\dot{V}(t)\tag{62}$$

because

$$\begin{aligned}\dot{V}(t) &= \sum_{i=1}^{\bar{n}}h_i(\varpi(t))D_{i1}\dot{x}_1(t)\\&= \sum_{i=1}^{\bar{n}}h_i(\varpi(t))D_{i1}(A_{i1}x_1(t)+B_{i1}u(t)+N_{i1}F_{tvs}(t))\end{aligned}\tag{63}$$

Therefore, by substituting equation (61) and (62) into (58), (64) can be obtained:

$$\begin{aligned}\frac{dJ}{dt} &= 2S_2(\mu-\mu_g)\int_a^b(y+c)\sum_{i=1}^{\bar{n}}h_i(\varpi(t))W_i dy\dot{V}(t)\\&\quad-S_1\int_a^b(\ln(\gamma(y+c,u(t)))+1)\sum_{i=1}^{\bar{n}}h_i(\varpi(t))W_i dy\dot{V}(t)\\&\quad+u(t)^TR\dot{u}(t)\end{aligned}\tag{64}$$

Construct the following controller:

$$\begin{aligned}u(t)^TR\dot{u}(t) &= -\lambda_{prey,c}\left|\mu-\mu_g\right|-2S_2(\mu-\mu_g)\int_a^b(y\\&\quad+c)\sum_{i=1}^{\bar{n}}h_i(\varpi(t))W_i dy\dot{V}(t)+S_1\int_a^b(\ln(\gamma(y\\&\quad+c,u(t)))+1)\sum_{i=1}^{\bar{n}}h_i(\varpi(t))W_i dy\dot{V}(t)\\&= -\lambda_{prey,c}\left|\mu-\mu_g\right|+(S_1\int_a^b(\ln(\gamma(y+c,u(t)))\\&\quad+1)\sum_{i=1}^{\bar{n}}h_i(\varpi(t))W_i dy-2S_2(\mu-\mu_g)\int_a^b(y\\&\quad+c)\sum_{i=1}^{\bar{n}}h_i(\varpi(t))W_i dy)\dot{V}(t)\end{aligned}\tag{65}$$

where $\lambda_{prey,c} > 0$, the following inequality holds:

$$\frac{dJ}{dt} = -\lambda_{prey,c}\left|\mu-\mu_g\right| < 0\tag{66}$$

Therefore, the closed-loop system is stable. □

The limited function $\lambda_{prey,c}$ is a proportional link, and can re-define the output steady-state value. It fuses fault estimation and observer residual information; the structure is as follows:

$$\lambda_{prey,c} = prey(\lambda)+\Gamma_3\varepsilon_n\tag{67}$$

The sensor fault produces an output mean transmission deviation, which causes the controller to use the received wrong mean as the judgment condition, so systems cannot accurately track the expected value. $\Gamma_3\varepsilon_n$ indirectly calibrates the transmission deviation and redefines the output steady-state value, hence passively compensates for sensor fault. The function with fault estimation information is $prey(\lambda)$ and its significance of active compensation are in Section III. C.

When there is no fault, according to Remark 2, Remark 4 and (41), c and ε_n can be ignored; the controller expression is as follows:

$$\begin{aligned}u(t)^TR\dot{u}(t) &= -prey(\lambda)\left|\mu-\mu_g\right|+[S_1\int_a^b(\ln(\gamma(y,u(t)))\\&\quad+1)\sum_{i=1}^{\bar{n}}h_i(\varpi(t))W_i dy-2S_2(\mu\end{aligned}$$

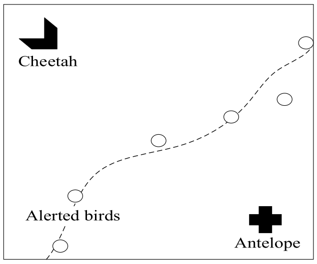

FIGURE 1. Positional relationship of two animals.

$$
-\mu_g)\int_a^b y\sum_{i=1}^{\bar{n}} h_i(\varpi(t))W_i dy]
\times D_{i1}(A_{i1}x_1(t)+B_{i1}u(t)) \quad (68)
$$

When only the sensor initial fault occurs, c and ε_n can be ignored. The controller expression is as follows:

$$
\begin{aligned}
u(t)^T R\dot{u}(t) = &-(prey(\lambda)+\Gamma_3\varepsilon_n)\left|\mu-\mu_g\right| + [S_1\int_a^b (\ln(\gamma(y \\
&+c, u(t)))+1)\sum_{i=1}^{\bar{n}} h_i(\varpi(t))W_i dy - 2S_2(\mu \\
&-\mu_g)\int_a^b (y+c)\sum_{i=1}^{\bar{n}} h_i(\varpi(t))W_i dy] \\
&\times D_{i1}(A_{i1}x_1(t)+B_{i1}u(t)) \qquad (69)
\end{aligned}
$$

When the actuator-sensor compound faults occur, the reconstructed controller expression is as follows:

$$
\begin{aligned}
u(t)^T R\dot{u}(t) = &-(prey(\lambda)+\Gamma_3\varepsilon_n)\left|\mu-\mu_g\right| + [S_1\int_a^b (\ln(\gamma(y \\
&+c, u(t)))+1)\sum_{i=1}^{\bar{n}} h_i(\varpi(t))W_i dy - 2S_2(\mu \\
&-\mu_g)\int_a^b (y+c)\sum_{i=1}^{\bar{n}} h_i(\varpi(t))W_i dy] \\
&\times D_{i1}(A_{i1}x_{1m}(t)+B_{i1}u_1(t)+N_{i1}\hat{F}_{tvs}(t)) \qquad (70)
\end{aligned}
$$

In summary, controller (56) utilizes the composite performance index to achieve the minimum-entropy FTC under unknown expected PDF conditions on the whole and implements the mean tracking control in concert.

C. PREY ALGORITHM

The prey algorithm is a variable-parameter method based on the predation game between cheetah and antelope. To judge the degree of threat from the cheetah and respond to it, an antelope can use the surrounding alerted birds. Based on this judgement, it can respond in two ways: run or continue to graze.

The idea of an antelope's response is related to the cheetah and birds. If the cheetah is slowly approaching, the distance is long, and the birds do not fly, then the antelope decides not to move. If the birds are alerted (i.e., they fly away), the antelope will become sensitive: if the cheetah is slowly approaching and the distance is short, then the antelope runs; if the cheetah runs and the distance is short, then the antelope keeps running. If the birds do not fly, the antelope will become insensitive: if the cheetah is slowly approaching and the distance is short, the antelope will not move; if the cheetah runs and the distance is short, then the antelope runs. Therefore, the prey strategy can be subdivided into sensitive and insensitive prey strategies based on the behavior of the birds; the correspondence is shown in Tables 1 and 2.

TABLE 1. Insensitive prey strategy.

Cheetah		*Antelope*	
Distance	*Status*	*Judgment*	*Response*
Far	Progressive	Safe	Static
Close	Progressive	Safe	Static
Close	Run	Threat	Run

TABLE 2. Sensitive prey strategy.

Cheetah		*Antelope*	
Distance	*Status*	*Judgment*	*Response*
Far	Progressive	Safe	Static
Close	Progressive	Threat	Run
Close	Run	Threat	Run

TABLE 3. FTC insensitive prey algorithm.

F_{tvs}		$u(t)$	
Distance	*Status*	*Judgment*	*Response*
$\chi\in(0, \tau_2]$	Fault free	Small impact	R_{i1}, λ_1
$\chi\in(\tau_2, 0.1\|B_i u^*(t)\|]$	Fault $F_{\sigma s,inc}$	Small impact	R_{i1}, λ_1
$\chi\in(0.1\|B_i u^*(t)\|, 0.5M]$	Fault $F_{\sigma s,non\text{-}inc}$	Big impact	R_{i2}, λ_2

TABLE 4. FTC insensitive prey algorithm.

F_{tvs}		$u(t)$	
Distance	*Status*	*Judgment*	*Response*
$\chi\in(0, \tau_2]$	Fault free	Small impact	R_{i1}, λ_1
$\chi\in(\tau_2, 0.1\|B_i u^*(t)\|]$	Fault $F_{\sigma s,inc}$	Big impact	R_{i2}, λ_2
$\chi\in(0.1\|B_i u^*(t)\|, 0.5M]$	Fault $F_{\sigma s,non\text{-}inc}$	Big impact	R_{i2}, λ_2

Replace the cheetah with F_{tvs}, the antelope with $u(t)$, and the birds with ε_n. Tables 3 and 4 show the corresponding relationship of the prey algorithm, where $R_{i1}, R_{i2}, \lambda_1$, and λ_2 are LMI-compliant adaptive learning rates and χ satisfies $\|F_{tvs}\| = \chi$.

The algorithm steps are as follows:

Step 1: Fault amplitude is less than or equal to τ_2, no fault, par- ameters are set to R_{i1}, λ_1.

Step 2: Fault amplitude is larger than τ_2 and less than or equal to $0.1\|B_i u^*(t)\|$, incipient fault, if feedback error integral is less than τ_1, parameters are insensitive and set to R_{i1}, λ_1.

Step 3: Fault amplitude is larger than τ_2 and less than or equal to $0.1\|B_i u^*(t)\|$, incipient fault, if feedback error integral is larger than or equal to τ_1, parameters are sensitive and set to R_{i2}, λ_2.

Step 4: Fault amplitude is larger than $0.1\|B_i u^*(t)\|$, large value fault, parameters are set to R_{i2}, λ_2.

Step 5: Return to Step 1 without modifying content.

From the prey algorithm, (20) and (67) can be summarized as

$$\begin{cases} \dot{\hat{F}}_{tvs}(t) = \sum_{i=1}^{\bar{n}} h_i(\varpi(t))(-prey(R_i)\hat{F}_{tvs}(t) + r_{i,c}\varepsilon_m(t)) \\ \lambda_{prey,c} = prey(\lambda) + \Gamma_3\varepsilon_n \end{cases} \quad (71)$$

where $prey(\cdot)$ is the adaptive switching law described as

$$prey(R_i,\lambda) = \begin{cases} R_{i1}, \lambda_1 & if\ \hat{\chi} \in (0, \tau_2] \\ R_{i1}, \lambda_1 & if\ \hat{\chi} \in (\tau_2, 0.1] \text{ and } \|\varepsilon_m\| \in [0, \tau_1) \\ R_{i2}, \lambda_2 & if\ \hat{\chi} \in (\tau_2, 0.1] \text{ and } \|\varepsilon_m\| \in [\tau_1, +\infty) \\ R_{i2}, \lambda_2 & if\ \hat{\chi} \in (0.1, 0.5M] \end{cases} \quad (72)$$

The systems can use the prey algorithm to achieve fast and accurate estimation of incipient actuator faults, while avoiding the interaction between sensor fault FTC and actuator faults FTC, ensuring the control performance.

IV. SIMULATION

In this section, a reentry hypersonic vehicle model with three inputs and single non-Gaussian stochastic output is used to verify the above methods. Similar models are often used for simulation verification to show the broad applicability of theory [13], [30]. For the systems described in (1) and (2), the output PDF can be approximated by the following B-spline $B_j(y)(j = 1, 2, 3)$:

$$B_1(y) = 0.5(y-2)^2 I_1 + (-y^2 + 7y - 11.5)I_2 + 0.5(y-5)^2 I_3 \quad (73)$$

$$B_2(y) = 0.5(y-3)^2 I_2 + (-y^2 + 9y - 19.5)I_3 + 0.5(y-6)^2 I_4 \quad (74)$$

$$B_3(y) = 0.5(y-4)^2 I_3 + (-y^2 + 11y - 29.5)I_4 + 0.5(y-7)^2 I_5 \quad (75)$$

where $I_\zeta(y)(\zeta = 1, \ldots, 5)$ represents the interval function, defined as

$$I_\zeta(y) = \begin{cases} 1, & y \in [\zeta+1, \zeta+2] \\ 0, & \text{otherwise.} \end{cases}$$

The deviation of the sensor fault appears in 20 s and is defined as

$$c = \begin{cases} 0.03\text{rand}(1), & t \in [0, 20s) \\ 0.98 + 0.03\text{rand}(1), & t \in [20s, +\infty) \end{cases} \quad (76)$$

where rand(1) is a random function that changes between 0 and 1 in MATLAB. We set an incipient random signal only to simulate the real environment; the controllers do not need to consider this.

Condition (35) in Assumption 2 ensures that the output $y + c$ of the sensor fault is in the integration interval $[a, b]$.

The nonlinearity of system is caused mainly by output weight v_1 in $V(t)$. v_1 has two related fuzzy sets $\{v_1 = 0.05\pi\}$ and $\{v_1 = 0.25\pi\}$; then, $i = 1, 2$, and the corresponding membership functions are given by

$$\begin{cases} h_1(v_1 = 0.05\pi) = (1 - \frac{1}{1+\exp(6-16v_1)}) \times \frac{1}{1+\exp(-6-16v_1)} \\ h_2(v_1 = 0.25\pi) = 1 - h_1(v_1 = 0.05\pi) \end{cases} \quad (77)$$

Thus, the fuzzy rules can be described as follows:

Rule 1: If v_1 is approximately 0.05π, then $i = 1$.

Rule 2: If v_1 is approximately 0.25π, then $i = 2$.

The linear modal parameter matrices in systems (1) and (2) are set as follows:

$$E = \begin{bmatrix} 1 & 0 & 0 \\ 0 & 1 & 0 \\ 0 & 0 & 0 \end{bmatrix}, \quad A_1 = \begin{bmatrix} 0.05 & 3.02 & -2.5 \\ -0.01 & 0 & 0.25 \\ 0 & -0.11 & 0.05 \end{bmatrix},$$

$$A_2 = \begin{bmatrix} 0.06 & 2.98 & -3.75 \\ -0.01 & 0 & 0.37 \\ 0.01 & -0.19 & 0.06 \end{bmatrix}, \quad B_1 = \begin{bmatrix} -2.9347 \\ -2.3109 \\ 2.1123 \end{bmatrix},$$

$$B_2 = \begin{bmatrix} -2.0618 \\ 2.2123 \\ 2.1006 \end{bmatrix}, N_1 = \begin{bmatrix} 0.5804 & 0.5804 & 0.5804 \\ 0.7715 & 0.7715 & 0.7715 \\ -0.3275 & -0.3275 & -0.3275 \end{bmatrix},$$

$$N_2 = \begin{bmatrix} 0.1721 & 0.1721 & 0.1721 \\ 0.0993 & 0.0993 & 0.0993 \\ -0.6198 & -0.6198 & -0.6198 \end{bmatrix},$$

$$D_1 = \begin{bmatrix} 0.1456 & -2.0671 & -6.9217 \\ 1.1488 & -0.7724 & 3.3891 \\ 0.2891 & -0.5067 & -2.6979 \end{bmatrix},$$

$$D_2 = \begin{bmatrix} 0.1456 & 0 & 0 \\ 0 & -0.7724 & 0 \\ 0 & 0 & -2.6979 \end{bmatrix},$$

$$U_1 = \begin{bmatrix} 0.4 & 0 & 0 \\ 0 & 0.8 & 0 \\ 0 & 0 & 1 \end{bmatrix}, U_2 = \begin{bmatrix} 1 & 0 & 0 \\ 0 & 0.8 & 0 \\ 0 & 0 & 0.4 \end{bmatrix}.$$

The desired mean is changed from 5 to 6 at 20 s. When $|u(t)| < 1$, the system parameter matrices can be transformed into an equivalent condition where $|u(t)| \geq 1$; the values of the parameter matrices have considered this equivalent. Select appropriate non-singular matrix P_i, Q_i and define the intermittent time-varying step actuator faults form as:

$$F_{tvs}(t) = [\,F1tvs(t) \quad F_{2tvs}(t) \quad F_{3tvs}(t)\,]^T \quad (78)$$

$$F_{1tvs}(t) = 2F_{2tvs}(t) = 4F_{3tvs}(t) \quad (79)$$

$$F_{1tvs}(t) = \begin{cases} F_{1\sigma}(t), & t \in (t_{\sigma 1}, t_{\sigma 2}] \\ 0, & otherwise \end{cases} \quad (80)$$

TABLE 5. Simulation comparison of performance for fault estimation.

Performance		New method	Traditional method
e_{ss1}	T2	0.0002	0.0717
	T3	0.0003	0.1242
	T4	0.0003	0.1093
e_{ss2}	T2	0.0003	0.0536
	T3	0.0004	0.1109
	T4	0.0004	0.1008
e_{ss3}	T2	0.0004	0.0671
	T3	0.0003	0.0935
	T4	0.0003	0.0822

By considering $\sigma_0 = 2$ and setting the fault window intervals, the fault assignment is given as

$$F_{1tvs}(t) = \begin{cases} F_{11}(t), & t \in (20s, 80s] \\ F_{12}(t), & t \in (100s, 160s] \\ 0, & otherwise \end{cases},$$

$$F_{11}(t) = \begin{cases} F_{11,inc}(t), & t \in (20s, 40s] \\ F_{11,non-inc}(t), & t \in (40s, 80s] \end{cases},$$

$$F_{12}(t) = \begin{cases} F_{12,inc}(t), & t \in (100s, 120s] \\ F_{12,non-inc}(t), & t \in (120s, 160s] \end{cases}.$$

According to the definition of incipient faults, B_1 and B_2, the actuator fault F_{1tvs} can be assigned twice:

$$\begin{cases} F_{11,inc}(t) = F_{12,inc}(t) = 0.2, \\ \qquad t \in (20s, 40s],\ (100s, 120s] \\ F_{11,non-inc}(t) = F_{12,non-inc}(t) = 1.2, \\ \qquad t \in (40s, 60s],\ (120s, 140s] \\ F_{11,non-inc}(t) = F_{12,non-inc}(t) = 1, \\ \qquad t \in (60s, 80s],\ (140s, 160s]. \end{cases}$$

Change from 1.2 to 1 is to simulate a superimposed actuator fault generated by the multi-electromagnetic interference sources in the superimposed interference interval. The remaining actuator faults also have this engineering background.

Table 5 and Table 6 show the performance comparison of our new method and the state-of-art in [31] in addressing multiple compound faults. These two tables show that the performance of the proposed method is stable and accurate. The traditional method does not have passive compensation and prey algorithms, so it is unable to estimate actuator faults especially incipient faults therein, the fault-tolerant tracking control of the mean cannot be realized.

In Table 5 and Table 6, e_{ss1}, e_{ss2}, and e_{ss3} are the steady-state estimation errors of F_{1tvs}, F_{2tvs}, and F_{3tvs}, respectively. $e_{ss,NF}$, $e_{ss,SF}$, and $e_{ss,CF}$ are the steady-state errors of mean tracking control under faultless, sensor fault, and compound fault conditions, respectively. T1, T2, T3, and T4 are the fault-free time (0–20 s), incipient fault time (20–40 s and 100–120 s), superimposed fault time (40–60 s and 120–140 s), and after-incipient fault time period (60–80 s and 140–160 s), respectively. Each value is the maximum value in the corresponding time period.

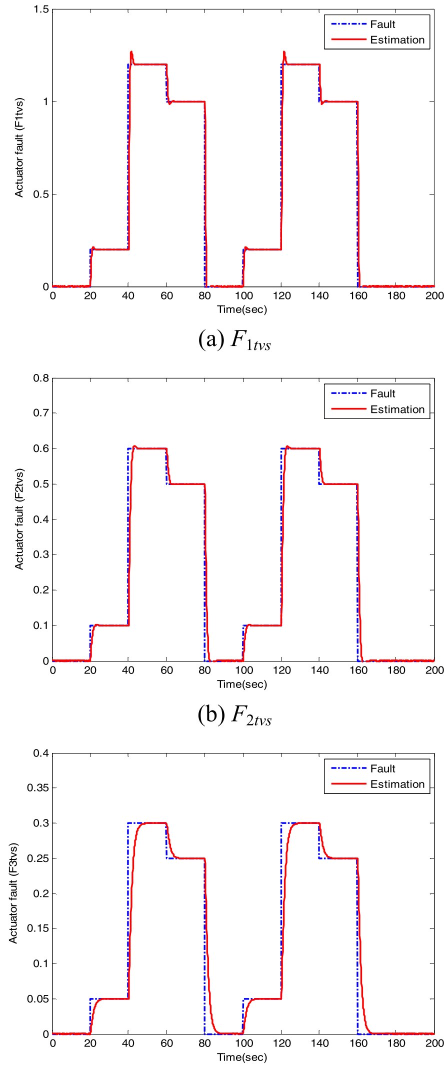

(a) F_{1tvs}

(b) F_{2tvs}

(c) F_{3tvs}

FIGURE 2. Actuator faults estimation.

TABLE 6. Simulation comparison of performance for FTC.

Performance		New method	Traditional method
$e_{ss,NF}$	T1	0.0001	0.0001
	T3	0.0002	0.0001
$e_{ss,SF}$	T1	0.0003	0.0003
	T3	0.0009	0.3643
$e_{ss,CF}$	T1	0.0003	0.0003
	T2	0.0004	0.2112
	T3	0.0007	0.4851
	T4	0.0007	0.4811

Figure 2–5 are simulation diagrams of the new method. Figure 2 shows the estimation of multiple actuator faults.

Figure 3 and Figure 4 show the FTC results under different fault conditions. The hybrid control scheme implements mean tracking control and minimum-entropy optimization.

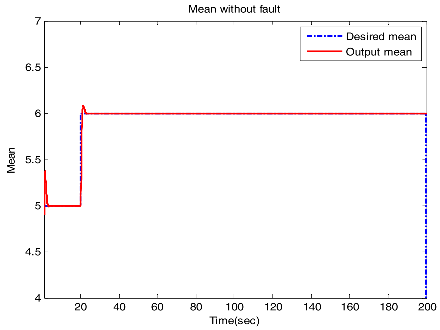

(a) No fault

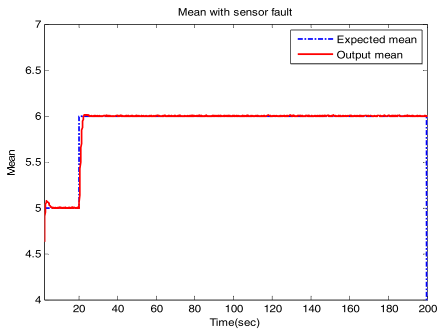

(b) Sensor fault

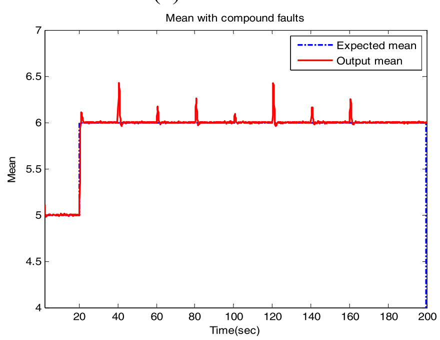

(c) Compound faults

FIGURE 3. **Mean tracking control of PDF.**

TABLE 7. **Gradual contrast of entropy under different indicators.**

Time	0.1s	1s	15s	85s	165s	195s
Ent1	2.6361	2.4007	2.3967	2.3959	2.3958	2.3958
Ent2	0.4543	0.4368	0.4339	0.4332	0.4331	0.4331

Entropy continues to decrease during the optimization, some progressive changes cannot be directly perceived from Figure 4. Table 7 shows the decrease at several moments. Ent1 and Ent2 are the optimizations without and with entropy indicators (J_1), respectively, the result of Ent2 is smaller and more ideal.

Figure 4 and Table 7 show that the entropy can reach the optimal interval in 1 s and continue to decrease to a small stable value under the reconstruction for compound faults. Thus, minimum-entropy control is achieved.

Figure 5 shows the output PDF. With the stabilization of the mean and entropy, finally the controller achieves

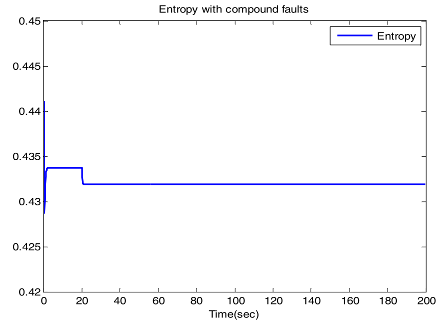

(a) No fault

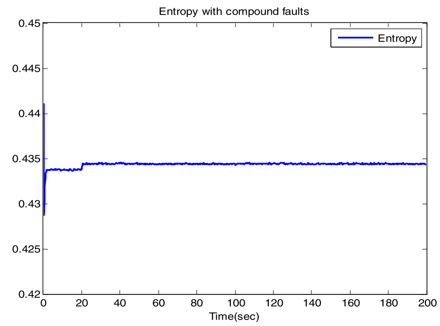

(b) Sensor fault

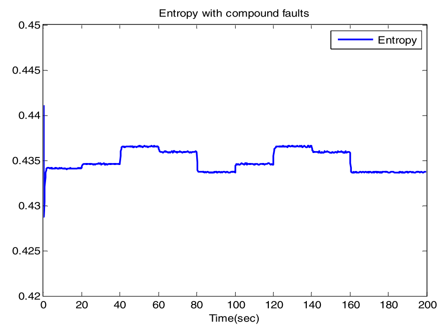

(c) Compound faults

FIGURE 4. **Optimal control of entropy.**

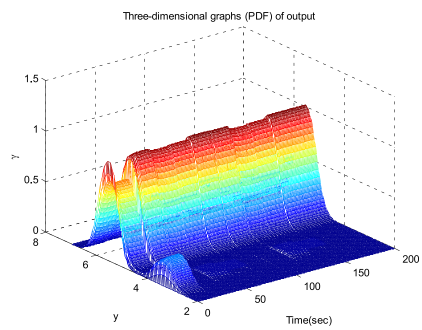

FIGURE 5. **3-dimensional output PDF.**

stable optimization of the output PDF shape. Therefore, the tracking control and minimum-entropy optimization with non-Gaussian stochastic outputs under compound faults are theoretically feasible.

V. CONCLUSION

The hybrid FTC scheme developed in this study effectively implements automatic repair of compound faults of non-Gaussian stochastic systems. The adaptive algorithm that mimics animal predation behavior is novel and intuitive. By combining the fuzzy premise variables with fault information in the prey algorithm, the controller has the ability to estimate and self-repair incipient faults. On this basis, the hybrid FTC scheme performed well in simulations: The actuator fault observer shields the sensor fault, and thus accurately estimates the incipient and large deviation actuator faults; the fault-tolerant controller uses a compensation function to passively shield the sensor fault, then actively repairs the actuator faults using estimation information. Then, the system accurately tracks the mean of the expected output PDF under every fault condition. The minimization of entropy is accompanied by the optimization of the performance indicator. Finally, by means of the fault-fuzzy information fusion and active-passive hybrid FTC scheme, non-Gaussian stochastic systems implement all objectives, including mean tracking control and minimum entropy optimization without an expected PDF.

ACKNOWLEDGMENT

We thank Kaiyu Hu's Ph.D. tutor Prof. Fuyang Chen for his guidance.

REFERENCES

[1] Y. Wang, S.-M. Yuan, D. Ling, Y.-B. Zhao, X.-G. Gu, and B. Y. Li, "Fault monitoring based on adaptive partition non-negative matrix factorization for non-Gaussian processes," *IEEE Access*, vol. 7, pp. 32783–32795, 2019.

[2] A. Kawasaki, T. Inakawa, J. Kasahara, K. Goto, K. Matsuoka, A. Matsuo, and I. Funaki, "Critical condition of inner cylinder radius for sustaining rotating detonation waves in rotating detonation engine thruster," *Proc. Combustion Inst.*, vol. 37, no. 3, pp. 3461–3469, Jun. 2019.

[3] H. Jamshidifar, S. Khosravani, B. Fidan, and A. Khajepour, "Vibration decoupled modeling and robust control of redundant cable-driven parallel robots," *IEEE/ASME Trans. Mechatronics*, vol. 23, no. 2, pp. 690–701, Apr. 2018.

[4] P. Lekha, T. Bush, N. Pammenter, P. Berjak, and B. Sitholè, "Quantitative assessment of xylan distribution across the secondary cell wall layers of Eucalyptus dissolving pulp fibres," *Holzforschung*, vol. 72, no. 1, pp. 1–8, Sep. 2018.

[5] C.-J. Bae, D.-C. Lee, and T. H. Nguyen, "Detection and identification of multiple IGBT open-circuit faults in PWM inverters for AC machine drives," *IET Power Electron.*, vol. 12, no. 4, pp. 923–931, Jan. 2019.

[6] L. Cao, D. Zhao, Y. Wang, and S. X. Ding, "Existence and design of observers for two-dimensional linear systems with multiple channel faults," *Multidimensional Syst. Signal Process.*, vol. 30, no. 2, pp. 641–660, Apr. 2019.

[7] A. Kodali, K. Pattipati, and S. Singh, "Coupled factorial hidden Markov models (CFHMM) for diagnosing multiple and coupled faults," *IEEE Trans. Syst., Man, Cybern. Syst.*, vol. 43, no. 3, pp. 522–534, May 2013.

[8] Z. G. Yi, N. Pan, and Y. Guo, "Mechanical compound faults extraction based on improved frequency domain blind deconvolution algorithm," *Mech. Syst. Signal Process.*, vol. 113, pp. 180–188, Dec. 2018.

[9] Q. K. Shen, B. Jiang, and P. Shi, "Adaptive fault diagnosis for T–S fuzzy systems with sensor faults and system performance analysis," *IEEE Trans. Fuzzy Syst.*, vol. 22, no. 2, pp. 274–285, Apr. 2014.

[10] V. Reppa, M. M. Polycarpou, and C. G. Panayiotou, "Decentralized isolation of multiple sensor faults in large-scale interconnected nonlinear systems," *IEEE Trans. Autom. Control*, vol. 60, no. 6, pp. 1582–1596, Jun. 2015.

[11] S. T. Wan, X. Zhang, and L. J. Dou, "Compound fault diagnosis of bearings using improved fast spectral kurtosis with VMD," *J. Mech. Sci. Technol.*, vol. 32, no. 11, pp. 5189–5199, Nov. 2018.

[12] W. Fan, Q. Zhou, J. Li, and Z. K. Zhu, "A wavelet-based statistical approach for monitoring and diagnosis of compound faults with application to rolling bearings," *IEEE Trans. Autom. Sci. Eng.*, vol. 15, no. 4, pp. 1563–1572, Oct. 2018.

[13] Q. Shen, B. Jiang, and V. Cocquempot, "Fault-tolerant control for T–S fuzzy systems with application to near-space hypersonic vehicle with actuator faults," *IEEE Trans. Fuzzy Syst.*, vol. 20, no. 4, pp. 652–665, Aug. 2012.

[14] J.-X. Zhang and G.-H. Yang, "Prescribed performance fault-tolerant control of uncertain nonlinear systems with unknown control directions," *IEEE Trans. Autom. Control*, vol. 62, no. 12, pp. 6529–6535, Dec. 2017.

[15] Q. Hu, X. Shao, and L. Guo, "Adaptive fault-tolerant attitude tracking control of spacecraft with prescribed performance," *IEEE/ASME Trans. Mechatronics*, vol. 23, no. 1, pp. 331–341, Feb. 2018.

[16] G. Li, T. Li, and Q. Zhao, "Fault tolerant shape control for particulate process systems under simultaneous actuator and sensor faults," *IET Control Theory Appl.*, vol. 11, no. 15, pp. 2448–2457, Oct. 2017.

[17] X. Li, D. Lu, G. Zeng, J. Liu, and W. Zhang, "Integrated fault estimation and non-fragile fault-tolerant control design for uncertain Takagi–Sugeno fuzzy systems with actuator fault and sensor fault," *IET Control Theory Appl.*, vol. 11, no. 10, pp. 1542–1553, Jun. 2017.

[18] S. Yin, H. Yang, and O. Kaynak, "Sliding mode observer-based FTC for Markovian jump systems with actuator and sensor faults," *IEEE Trans. Autom. Control*, vol. 62, no. 7, pp. 3551–3558, Jul. 2017.

[19] H. Chen, B. Jiang, W. Chen, and H. Yi, "Data-driven detection and diagnosis of incipient faults in electrical drives of high-speed trains," *IEEE Trans. Ind. Electron.*, vol. 66, no. 6, pp. 4716–4725, Jun. 2019.

[20] K. Zhang, B. Jiang, X.-G. Yan, and J. Shen, "Interval sliding mode observer based incipient sensor fault detection with application to a traction device in China railway high-speed," *IEEE Trans. Veh. Technol.*, vol. 68, no. 3, pp. 2585–2597, Mar. 2019.

[21] E. Li, L. N. Wang, and B. Song, "Fault diagnosis of power transformers with membership degree," *IEEE Access*, vol. 7, pp. 28791–28798, 2019.

[22] L. Li, H. Luo, S. X. Ding, Y. Yang, and K. X. Peng, "Performance-based fault detection and fault-tolerant control for automatic control systems," *Automatica*, vol. 99, pp. 308–316, Jan. 2019.

[23] D. Zhao, H. R. Karimi, R. Sakthivel, and Y. Li, "Non-fragile fault-tolerant control for nonlinear Markovian jump systems with intermittent actuator fault," *Nonlinear Anal., Hybrid Syst.*, vol. 32, pp. 337–350, May 2019.

[24] S. Y. Hu, L. Wang, J. M. Mao, C. Gao, B. Zhang, and S. S. Yang, "Synchronous online diagnosis of multiple cable intermittent faults based on chaotic spread spectrum sequence," *IEEE Trans. Ind. Electron.*, vol. 66, no. 4, pp. 3217–3226, Apr. 2019.

[25] J. Zhang, P. D. Christofides, X. He, Z. Wu, Z. Zhang, and D. Zhou, "Event-triggered filtering and intermittent fault detection for time-varying systems with stochastic parameter uncertainty and sensor saturation," *Int. J. Robust Nonlinear Control*, vol. 28, no. 16, pp. 4666–4680, Nov. 2018.

[26] S. Sun, H. Zhang, Y. Wang, and Y. Cai, "Dynamic output feedback-based fault-tolerant control design for T-S fuzzy systems with model uncertainties," *ISA Trans.*, vol. 81, pp. 32–45, Oct. 2018.

[27] X. Xu, Y. Zhang, M. Ren, J. Zhang, and G. Yan, "Generalized correntropy filter-based fault diagnosis and tolerant control for non-Gaussian stochastic systems subject to sensor faults," *IEEE Access*, vol. 6, pp. 12598–12607, 2016.

[28] L. N. Yao and C. H. Lei, "Fault diagnosis and sliding mode fault tolerant control for non-Gaussian stochastic distribution control systems using T-S fuzzy model," *Asian J. Control*, vol. 19, no. 2, pp. 636–646, Mar. 2017.

[29] L. N. Yao and L. Feng, "Fault diagnosis and fault tolerant tracking control for the non-Gaussian singular time-delayed stochastic distribution system with PDF approximation error," *Neurocomputing*, vol. 175, no. 2, pp. 538–543, Jun. 2016.

[30] L. N. Yao and L. Feng, "Fault diagnosis and fault tolerant control for the non-Gaussian time-delay singular stochastic distribution system," *Int. J. Control Autom. Syst.*, vol. 14, no. 2, pp. 435–442, Apr. 2016.

[31] H. K. Jin, Y. Guan, and L. Yao, "Minimum entropy active fault tolerant control of the non-Gaussian stochastic distribution system subjected to mean constraint," *Entropy*, vol. 19, no. 5, pp. 218–232, May 2017.

[32] J. Zhou, H. Yue, and H. Wang, "Shaping of output PDF based on the rational square-root b-spline model," *Acta Autom. Sinica*, vol. 31, no. 3, pp. 343–351, May 2005.

KAIYU HU received the B.E. degree in automation from Jilin University, Changchun, China, in 2012, and the M.S. degree in astrophysics from the University of Chinese Academy of Sciences, Beijing, China, in 2015. He is currently pursuing the Ph.D. degree with the Nanjing University of Aeronautics and Astronautics, Nanjing, China.

His research interests include adaptive control, non-Gaussian systems, and fault-tolerant control.

FUYANG CHEN received the D.E. degree in automation engineering from the Nanjing University of Aeronautics and Astronautics, Nanjing, China, in 2013, where he is currently with the College of Automation Engineering.

He has strong research, teaching, and engineering skills. His research interests include adaptive control, flight control, quantum control, and self-repairing control.

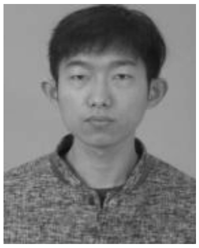

ZIAN CHENG was born in Xuzhou, Jiangsu, China. He graduated from Southwest Forestry University, Kunming, Yunnan, China. He is currently pursuing the Ph.D. degree with the Nanjing University of Aeronautics and Astronautics, Nanjing, China.

He has extensive experience in software design. His research interests include adaptive control, guaranteed performance control, and fault-tolerant tracking control for hypersonic flight vehicle.

CHANGYUN WEN received the B.Eng. degree from Xi'an Jiaotong University, in July 1983, and the Ph.D. degree from the University of Newcastle, Australia, in February 1990.

From August 1989 to August 1991, he was a Research Associate and then a Postdoctoral Fellow with the University of Adelaide, Australia. Then, he joined the School of Electrical and Electronic Engineering, Nanyang Technological University, as a Lecturer. He was promoted to Full Professor through the first promotion and tenure review exercise at NTU, in 2008. His main research interests include adaptive control, intelligent power management systems for more electric aircraft, modeling and control of active chilled beam for HVAC systems, switching and impulsive systems, and model-based online learning.